

Spectroscopic evidence for many body effects in the superconducting state of $\text{Bi}_2\text{Sr}_2\text{CaCu}_2\text{O}_{8+\delta}$

A. Kaminski,^{1,2} M. Randeria,³ J. C. Campuzano,^{1,2} M. R. Norman,² H. Fretwell,⁴ J. Mesot,⁵ T. Sato,⁶ T. Takahashi,⁶ K. Kadowaki⁷

(1) *Department of Physics, University of Illinois at Chicago, Chicago, IL 60607*

(2) *Materials Sciences Division, Argonne National Laboratory, Argonne, IL 60439*

(3) *Tata Institute of Fundamental Research, Mumbai 400005, India*

(4) *Department of Physics, University of Wales Swansea, Swansea SA2 8PP, UK*

(5) *Laboratory for Neutron Scattering, ETH Zurich and PSI Villigen, CH-5232 Villigen PSI, Switzerland*

(6) *Department of Physics, Tohoku University, 980 Sendai, Japan*

(7) *Institute of Materials Science, University of Tsukuba, Ibaraki 305, Japan*

Angle-resolved photoemission (ARPES) data in the superconducting state of $\text{Bi}_2\text{Sr}_2\text{CaCu}_2\text{O}_{8+\delta}$ show a kink in the dispersion along the zone diagonal, which is related via a Kramers-Krönig analysis to a drop in the low-energy scattering rate. As one moves towards $(\pi, 0)$, this kink evolves into a spectral dip. The occurrence of these anomalies in the dispersion and lineshape throughout the zone indicate the presence of a new energy scale in the superconducting state.

74.25.Jb, 74.72.Hs, 79.60.Bm

The high temperature superconductors exhibit many unusual properties, one of the most striking being the linear dependence of the resistivity on temperature in the normal state. This behavior has been attributed to the presence of a quantum critical point, where the only relevant energy scale is the temperature [1]. However, new energy scales become manifest below T_c due to the appearance of the superconducting gap and resulting collective excitations. Thus one would in general not expect response functions to continue to exhibit ω/T scaling in the superconducting state. The effect of these new scales on the ARPES spectral function below T_c have been well studied near the $(\pi, 0)$ point of the zone [2,3]. In this Letter we show how these scales manifest themselves in the spectral functions over the entire Brillouin zone. In particular, they have important consequences even on the zone diagonal where the gap vanishes.

We find that there are significant changes in both the lineshape and dispersion of the spectra below T_c , relative to the normal state where the nodal points exhibit quantum critical scaling [4]. Specifically, below T_c there is a velocity renormalization (by about a factor of 2) along the zone diagonal which sets in at a finite energy (~ 70 meV). This is accompanied, as required by Kramers-Krönig relations, by a reduction in the linewidth leading to well-defined quasiparticles. As one moves away from the node, the velocity renormalization increases, and the kink in dispersion along the diagonal smoothly evolves into the spectral dip [2], with the same characteristic energy scale throughout the zone. We will argue that this energy scale is caused by the magnetic resonance observed directly by neutron scattering [5].

We begin our analysis by recalling [6] that, within the impulse approximation, the ARPES intensity for a

quasi-two-dimensional system is given by [7] $I(\mathbf{k}, \omega) = I_0(\mathbf{k})f(\omega)A(\mathbf{k}, \omega)$. Here \mathbf{k} is the in-plane momentum, ω is the energy of the initial state relative to the chemical potential, f is the Fermi function, I_0 is proportional to the dipole matrix element $|M_{fi}|^2$, and A is the one-particle spectral function. Fig. 1 shows data [8] as a function of \mathbf{k} and ω .

$A(\mathbf{k}, \omega) = (-1/\pi)\Im mG(\mathbf{k}, \omega + i0^+)$ can be written as

$$A(\mathbf{k}, \omega) = \frac{1}{\pi} \frac{|\Sigma''(\mathbf{k}, \omega)|}{[\omega - \epsilon_{\mathbf{k}} - \Sigma'(\mathbf{k}, \omega)]^2 + [\Sigma''(\mathbf{k}, \omega)]^2}. \quad (1)$$

where the self-energy $\Sigma = \Sigma' + i\Sigma''$ and $\epsilon_{\mathbf{k}}$ is the bare dispersion. For \mathbf{k} near k_F , and varying normal to the Fermi surface (shown in the inset in Fig. 1), we may write $\epsilon_{\mathbf{k}} \simeq v_F^0(k - k_F)$, where both $k_F(\theta)$ and the bare Fermi velocity $v_F^0(\theta)$ depend in general on the angle θ along the Fermi surface.

In Fig. 2a, we plot the dispersion of the spectral peak above T_c obtained from constant \mathbf{k} scans (energy distribution curves or EDCs), and the peak in momentum obtained from constant ω scans (momentum distribution curves or MDCs) [4] from data similar to Fig. 1. We find that the EDC and MDC peak dispersions are very different, a consequence of the ω dependence of Σ . To see this, we note from Eq. (1) that the MDC at fixed ω is a Lorentzian centered at $k = k_F + [\omega - \Sigma'(\omega)]/v_F^0$, with a width (HWHM) $W_M = |\Sigma''(\omega)|/v_F^0$, provided (i) Σ is essentially independent [9] of k normal to the Fermi surface, and (ii) the dipole matrix elements do not vary significantly with k over the range of interest. That these two conditions are fulfilled can be seen by the nearly Lorentzian MDC lineshape of the data plotted in Fig. 1b.

On the other hand, the EDC at fixed \mathbf{k} (Fig. 1c) has a non-Lorentzian lineshape reflecting the non-trivial

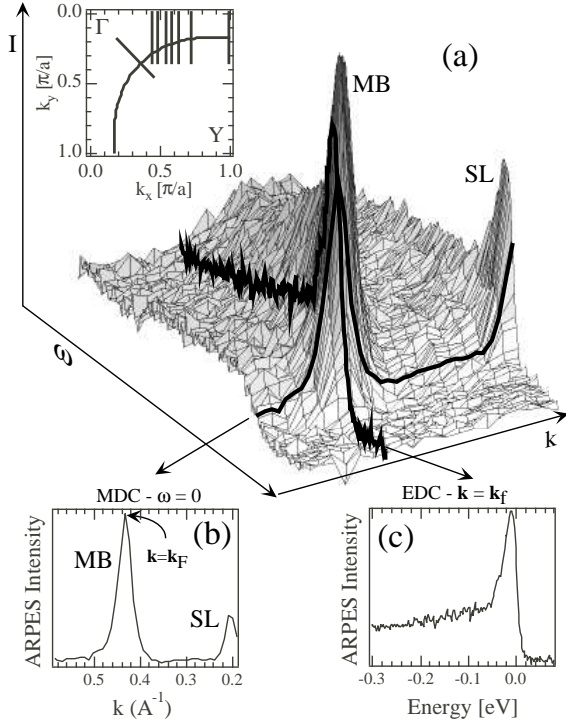


FIG. 1. (a) The ARPES intensity as a function of \mathbf{k} and ω at $h\nu=22\text{eV}$ and $T=40\text{K}$. MB is the main band, and SL a superlattice image. (b) a constant ω cut (MDC) from (a). (c) a constant \mathbf{k} cut (EDC) from (a). The diagonal line in the zone inset shows the location of the \mathbf{k} cut (the curved line is the Fermi surface).

ω -dependence of Σ'' , in addition to the Fermi cutoff at low energies. Thus the EDC peak is *not* given by $[\omega - v_F^0(k - k_F) - \Sigma'(\omega)] = 0$ but also involves Σ'' , unlike the MDC peak. Further, a very rough estimate of the EDC width (HWHM) is given by $W_E = |\Sigma''(E_k)|/[1 - \partial\Sigma'/\partial\omega|_{E_k}]$, where E_k is the peak position.

We thus see that it is much simpler to interpret the MDC peak positions, and consequently focus on the change in the MDC dispersion going from the normal (N) to the superconducting (SC) state shown in Fig. 2b. The striking feature of Fig. 2b is the development of a kink in the dispersion below T_c . At fixed ω let the dispersion change from k_N to k_{SC} . Using $v_F^0(k_N - k_{SC}) = \Sigma'_{SC}(\omega) - \Sigma'_N(\omega)$, we directly obtain the change in real part of Σ plotted in Fig. 2c. The Kramers-Krönig transformation of $\Sigma'_{SC} - \Sigma'_N$ then yields $\Sigma''_N - \Sigma''_{SC}$, plotted in Fig. 2d, which shows that $|\Sigma''_{SC}|$ is smaller than $|\Sigma''_N|$ at low energies.

We compare these results in Fig. 3a with the $W_M = |\Sigma''|/v_F^0$ estimated directly from the MDC Lorentzian linewidths. The normal state curve was obtained from a linear fit to the corresponding MDC width data points in Fig. 3a, and then the data from Fig. 2d was added to it to generate the low temperature curve. We are thus able to make a quantitative connection between the appearance

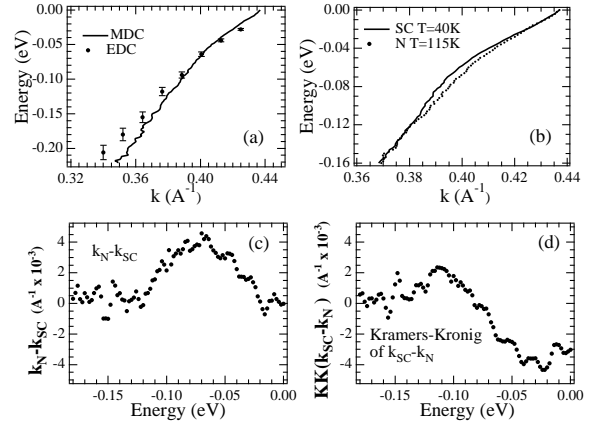


FIG. 2. ARPES data along the (π, π) direction at $h\nu=28\text{eV}$. (a) EDC dispersion in the normal state compared to the MDC dispersion. The EDCs are shown in Fig. 3d. (b) MDC dispersions in the superconducting state ($T=40\text{K}$) and normal state ($T=115\text{K}$). (c) change in MDC dispersion from (b). (d) Kramers-Krönig transform of (c).

of a kink in the (MDC) dispersion below T_c and a drop in the low energy scattering rate in the superconducting state relative to the normal state. We emphasize that we have estimated these T -dependent changes in the complex self-energy without making fits to the EDC lineshape, thus avoiding the problem of modeling the ω dependence of Σ and the extrinsic background.

One can also analyze the data by starting with the linewidths and deducing changes in the dispersion. The ratio of the EDC (obtained from Fig. 3d) and MDC widths is given by $W_E/W_M = v_F^0/[1 - \partial\Sigma'/\partial\omega] = v_F$, the renormalized Fermi velocity. One can see a sudden drop in velocity around 70 meV, from $\approx 2.5 \text{ eV\AA}$ above to $\approx 1.5 \text{ eV\AA}$ below 70 meV. This results in a sharp kink in the dispersion, which can be directly seen in the raw data shown in Fig. 4.

Notice that we have completed a full circle. Starting with the change in MDC dispersion, we deduced the change in MDC width. Dividing the EDC by the MDC width, we deduced the velocity renormalization. This remarkable connection between different aspects of the data reveals the full power of analyticity and causality in many-body theory.

The reduction in $|\Sigma''|$ below T_c reflects a drop in the scattering rate. We now ask ourselves how this drop in the scattering rate evolves as we move along the Fermi surface. Away from the node a quantitative analysis (like the one above) becomes more complicated [11] and will be presented in a later publication. Here, we will simply look at the evolution of the dispersion. In Fig. 4, we plot raw (2D) data as obtained from our detector for a series of cuts parallel to the MY direction (normal state in left panels, superconducting state in middle panels). We start from the bottom row that corresponds

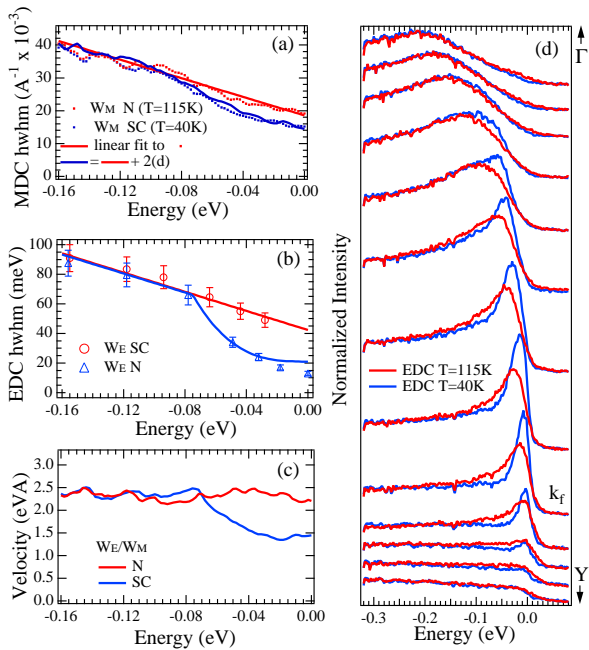


FIG. 3. (a) Comparison of change in Σ'' obtained directly from the MDC widths (HWHM) to the one obtained from the dispersion in Fig. 2d by using the Kramers-Krönig transform. (b) HWHM width obtained from EDCs shown in (d). Lines marked by fit are linear in normal state and linear/cubic in superconducting state. The data in (b) fall below the fits at low energies because of the Fermi cut-off of the EDCs. (c) Renormalized velocity obtained from dividing (b) by (a).

to a cut close to the node and reveals the same kink described above. As we move towards $(\pi, 0)$, the dispersion kink (middle panels) becomes more pronounced and at around $k_x=0.55$ develops into a break separating the faster dispersing high energy part of the spectrum from the slower dispersing low energy part. This break leads to the appearance of two features in the EDCs, shown in the right panels of Fig. 4. Further towards $(\pi, 0)$, the low energy feature (the quasiparticle peak) becomes almost dispersionless. At the $(\pi, 0)$ point, this break effect becomes the most pronounced, giving rise to the well known peak/dip/hump structure.

We note that the evolution of the dispersion from kink to break occurs continuously, at the exact same energy of 70-80 meV. We must therefore conclude that they are in fact of the same origin. As discussed earlier, the most natural explanation of this effect near $(\pi, 0)$ is in terms of electrons interacting with a collective mode [2] below T_c , whose energy and characteristic wavevector matches [3] the sharp magnetic resonance observed directly by neutron scattering. Since the break evolves smoothly from the kink, and sets in at the same energy, we are led to the conclusion that the same collective mode effect dominates the superconducting lineshape at all points in the zone, including the node [12]. In essence, there is a suppression of the low energy scattering rate due to the finite

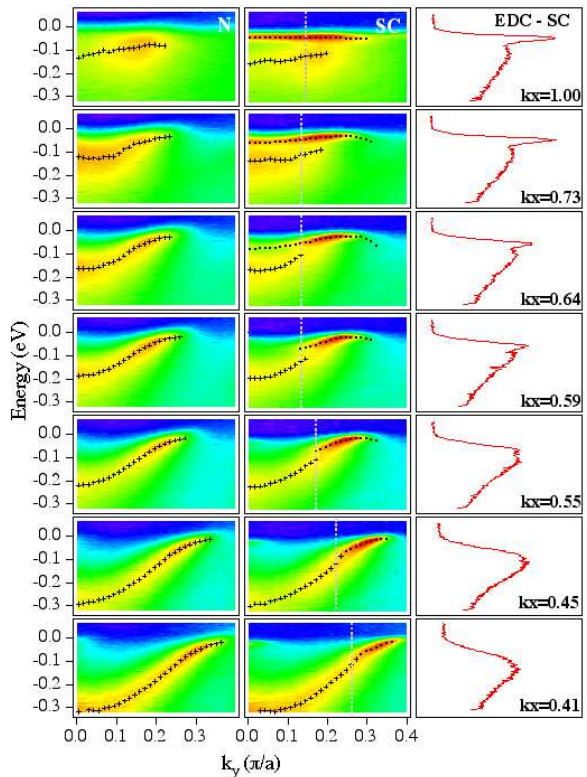


FIG. 4. Left panels: Log of normal state ($h\nu=22\text{eV}$, $T=140\text{K}$) ARPES intensity along selected cuts (shown in zone inset in Fig. 1). EDC peak positions are indicated by crosses. Middle panels: Log of superconducting state ($T=40\text{K}$) intensity at the same cuts as for left panels. Crosses indicate positions of broad high energy peaks, dots sharp low energy peaks. Right panels: EDCs at locations marked by the vertical lines in the middle panels.

energy of the mode.

We now examine in greater detail the lineshape as a function of momentum. Since the neutron mode is characterized by a (π, π) wavevector, one would expect its effect on the lineshape to be much stronger at points in the zone which are spanned by (π, π) [13]. This is indeed the case, as can be seen in Fig. 5. Near the node, the drop in the scattering rate is such that it causes a kink in the dispersion. But upon approaching the $(\pi, 0)$ point, the drop in Σ'' is so drastic as to produce a dip in the spectral function. At this point we can only put bounds on how fast Σ'' drops. Near the node it drops slower than ω^3 (see Fig. 3), while near $(\pi, 0)$ it must drop at least as fast as ω^6 [14]. In Fig. 5 we have drawn a line at 80 meV, the energy at which the drop in Σ'' occurs. A glance at the EDCs emphasizes the fact that the drop in scattering rate occurs throughout the zone. The energy at which the drop occurs is consistent with our previous work, since it is seen in the EDC at an energy equal to the sum [15] of the mode energy Ω_0 and the maximum gap Δ_0 , both of which are ≈ 40 meV for optimally doped samples. It is

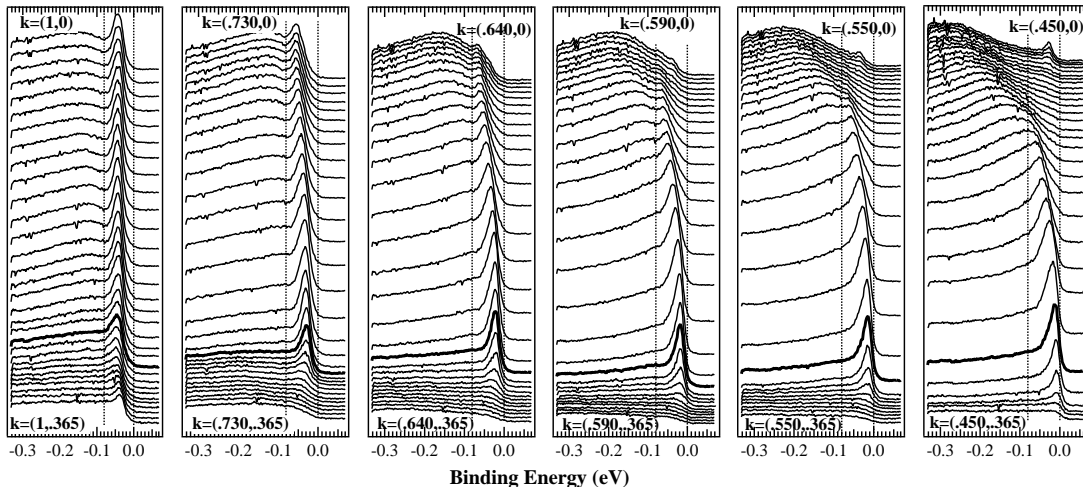


FIG. 5. ARPES intensity ($T=40\text{K}$) along selected cuts from Fig. 4. The thick lined curves correspond approximately to \mathbf{k}_F . Vertical lines are at 0 and -80 meV .

the presence of this finite energy scale which leads to deviations from the normal state quantum critical scaling below T_c .

In summary, we have shown by a simple, self-consistent analysis based on general properties of the spectral function and self-energy, that $\text{Bi}_2\text{Sr}_2\text{CaCu}_2\text{O}_{8+\delta}$ shows a velocity renormalization along the zone diagonal which is directly related to a drop in the low energy scattering rate below T_c . The anomalies in the dispersion and lineshape evolve smoothly as one moves from the zone diagonal to the zone corner, but always show the same characteristic energy scale. We suggest that this suppression of the scattering rate below T_c at all points in the Brillouin zone is due to the presence of a gap and a finite energy collective mode, which we identify with the magnetic resonance observed by neutron scattering.

This work was supported by the National Science Foundation DMR 9974401, the U. S. Dept. of Energy, Basic Energy Sciences, under contract W-31-109-ENG-38, the CREST of JST, and the Ministry of Education, Science, and Culture of Japan. The Synchrotron Radiation Center is supported by NSF DMR 9212658. JM is supported by the Swiss National Science Foundation, and MR in part by the Indian DST through the Swarnajayanti scheme.

Note added. After completion of this work, we became aware of related work by Bogdanov *et al.*, condmat/0004349.

- [2] M. R. Norman *et al.*, Phys. Rev. Lett. **79**, 3506 (1997); M. R. Norman and H. Ding, Phys. Rev. B **57**, R11089 (1998).
- [3] J.C. Campuzano *et al.*, Phys. Rev. Lett. **83**, 3709 (1999).
- [4] T. Valla *et al.*, Science **285**, 2110 (1999).
- [5] H. F. Fong *et al.*, Nature **398**, 588 (1999).
- [6] M. Randeria *et al.*, Phys. Rev. Lett. **74**, 4951 (1995).
- [7] The experimental signal is a convolution of this with the energy resolution and a sum over the momentum window, plus an additive (extrinsic) background.
- [8] The optimally doped $\text{Bi}_2\text{Sr}_2\text{CaCu}_2\text{O}_{8+\delta}$ ($T_c=90\text{K}$) samples were grown using the floating zone method. The samples were mounted with either the ΓX or ΓM axis parallel to the photon polarization vector, and cleaved in situ at pressures less than $5 \cdot 10^{-11}$ Torr. We used a Scienta SES 200 electron analyzer with energy resolution of 16 meV and a momentum resolution of 0.0097 \AA^{-1} . Measurements were carried out at the Synchrotron Radiation Center in Madison WI, on the U1 undulator beamline supplying 10^{12} photons/sec.
- [9] Note that: (1) a linear dependence of Σ' on $k - k_F$ can be absorbed into the definition of v_F^2 ; (2) Σ has an implicit dependence on θ .
- [10] A. Kaminski *et al.*, Phys. Rev. Lett. **84**, 1788 (2000).
- [11] Such an analysis would need to include (1) the superconducting gap which affects Σ through a pairing contribution; (2) the quadratic dispersion about the ΓM symmetry line, which is close to E_F near $M = (\pi, 0)$.
- [12] Similar kinks have been seen in ARPES in normal metals due to phonons, see M. Hengsberger *et al.*, Phys. Rev. Lett. **83**, 592 (1999); T. Valla *et al.*, *ibid.*, 2085 (1999).
- [13] Z.-X. Shen and J. R. Schrieffer, Phys. Rev. Lett. **78**, 1771 (1997).
- [14] M. R. Norman *et al.*, Phys. Rev. B **60**, 7585 (1999).
- [15] As discussed in ref. [3], the different doping dependences of Ω_0 and Δ_0 can be used to discriminate between $2\Delta_0$ and $\Omega_0 + \Delta_0$ which happen to coincide near optimality.

[1] B. Batlogg and C. M. Varma, Physics World, Feb., p. 33 (2000).